Microbial Fuel Cell Driven Behavioral Dynamics in Robot Simulations

Alberto Montebelli[1], Robert Lowe[1], Ioannis Ieropoulos[2], Chris Melhuish[2], John Greenman[3] and Tom Ziemke[1]

[1]Cognition & Interaction Lab, University of Skövde, Sweden
[2]Bristol Robotics Laboratory, University of Bristol and University of the West of England, UK
[3]Microbiology Research Lab, University of the West of England, UK
alberto.montebelli@his.se

Abstract

With the present study we report the first application of a recently proposed model for realistic microbial fuel cells (MFCs) energy generation dynamics, suitable for robotic simulations with minimal and extremely limited computational overhead. A simulated agent was adapted in order to engage in a viable interaction with its environment. It achieved energy autonomy by maintaining viable levels of the critical variables of MFCs, namely cathodic hydration and anodic substrate biochemical energy. After unsupervised adaptation by genetic algorithm, these crucial variables modulate the behavioral dynamics expressed by viable robots in their interaction with the environment. The analysis of this physically rooted and self-organized dynamic action selection mechanism constitutes a novel practical contribution of this work. We also compare two different viable strategies, a self-organized continuous and a pulsed behavior, in order to foresee the possible cognitive implications of such biological-mechatronics hybrid symbionts in a novel scenario of *ecologically grounded* energy and motivational autonomy.

Introduction

Over the past decade, the perspective on what constitutes adaptive behavior in living organisms and robots has evolved from one of embodiment entailing solely the study of sensorimotor activity to one that incorporates internal bodily dynamics (e.g. Pfeifer and Scheier, 1999; Wilson, 2002; Ziemke, 2003). This century, the increased emphasis on internal dynamics to behavior has led some researchers to suggest that non-neural activity – of the type that is substantially affected by whole organism interaction with an external environment – is indispensable for garnering further insights into the nature of adaptive behavior (cf. Parisi, 2004; Ziemke, 2008; Ziemke and Lowe, 2009). Furthermore, the integration between non-neural internal components and sensorimotor activity may be at the heart of related concepts such as autonomy, emotion and agency.

The importance of non-neural internal (bodily) variables to behavioral dynamics was well appreciated by Ashby (1960). A leading figure in the British cybernetics movement in the 40s and 50s, Ashby emphasized the importance of feedback to control systems and, drawing on the work of Cannon (1915), applied the biological notion of homeostasis to an engineered artifact, the *homeostat*. The essential cognitive feature of the homeostat is that it purportedly provides a demonstration of what makes a system truly adaptive, or *ultrastable*. According to Ashby, a requisite feature of adaptive living and artificial organisms is that their behavior is governed not just by a first order reactive sensorimotor loop but also by a second order loop. In the case where environmental changes occur such that the value of a set of *essential variables* (e.g. blood glucose level) deviate from an ideal/viable bounded region, the 2nd order loop may be enacted. This 2nd order loop entails random changes in some of the system parameters that affect organism-environment interactive coupling, i.e. inducing a remapping of the sensorimotor activity. Only when the reconfiguration of the parameter values, altering the sensorimotor activity, permits essential variable values to be re-established within their ideal bounds, the stable/viable organism-environment interactive coupling will be likewise re-established.

Robotics investigations and research into adaptive simulated agents has been increasingly embracing the role of bodily dynamics regarding autonomous and adaptive behavior. Robot controllers utilizing homeostatic and non-neural modulatory mechanisms for cognitive shaping have been applied to navigation problems (Moioli et al., 2008, – neuroendocrine control), foraging (McHale and Husbands, 2006, – system-level energy constraints), competitive two-resource problems (Avila-García and Cañamero, 2004, – synthetic hormones). Other minimalist and dynamic systems centred approaches have investigated the effects of 'energy' or 'essential variables' that link agent viability to adaptive environmental interactions in terms of: action selection and anticipation (Montebelli et al., 2008, 2009), environment-contingent 'bodily' monitoring (Saglimbeni and Parisi, 2009), internal expression in resource competitive scenarios (Lowe et al., 2005) and also with regard to a minimal cognitive robotics interpretation of Ashby's ultrastability concept (Di Paolo, 2003). This whole body of work, relevant to system level energy constraints and neuro-physiological homeostatic control, has invariably

assumed abstract (or even arbitrary) metabolic dynamics. The homeostatic dynamics and their impact on robot behavior is rooted in designer-specified requirements and means of fulfillment, rather than on any bio-chemical reality.

A real-world instantiation of 'artificial metabolism', that can provide wheeled robots with (electrical) energy for behavioral performance as constrained by actual bio-chemical essential variable dynamics, exists in the form of Microbial Fuel Cell (MFC) technology (cf. Melhuish et al., 2006; Ieropoulos et al., 2007; Logan et al., 2006). MFC technology has the capacity to produce bioelectricity from virtually any unrefined renewable biomass (e.g. wastewater sludge, ripe fruit, flies, green plants) using bacteria. This provides robots with a degree of energy autonomy concerning choice of (non-battery) 'energy recharging' resource. Individual cells consist of anode and cathode compartments. Owing to the need for persistent rehydration of the electrode in the cathode compartment and the provision of substrate to be 'metabolized' in the anode compartment, the MFC electric energy wielding power can be said to depend on the dynamics of biochemical energy and water, essential variables of the system. Ongoing work in this area has led to generations of this MFC-powered robot demonstrating increasing independence from outside (human) control. The present incarnation EcoBot-III, for example, is able to circulate water and substrate intake according to a number of actuators (pumps) that also require a modicum of electric energy 'overhead'. Given the present state of the art, a critical limitation of this robot, motored by a biological-mechatronic symbiotic metabolism, is energy requirement. Individual robots are required to wait long-intervals between bursts of motor activity. Many minutes may be required for relatively little movement. Simulations based scenarios offer a means to overcome such performance constraints whilst simultaneously providing a tool for offering new insights and future direction. Moreover, the application of a (simulated) physically constrained metabolic dynamic on robotic behavioral competences, offers opportunities for investigating the significance of forms of homeostatic dynamics, provisioning adaptive behavior as it emerges from sensorimotor, internal and agent-environment interactions.

In the remainder of this article we will firstly present a MFC model pitted at a level of abstraction suitable for relative robotic platform independence and mathematically described. Secondly, we describe an abstract experimental scenario, and methodological approach used, in which a simulated robot is required to balance its MFC essential variable levels in order to remain viable. Thirdly, we report results from this experiment according to the evolutionary emergence of sensorimotor strategies tightly coupled to essential variable needs and environmental resource availability. Finally, we provide a discussion on the potential for simulations-based MFC-robotics applications to uncovering new breakthroughs in the physical domain.

Method

The MFC model

The core element of our experimental setup is constituted by the model of MFC recently reported by Montebelli et al. (2010a). The model has been derived from real experimental data generated by EcoBot-II, a prototype robot developed at the Bristol Robotics Lab and described in detail in Melhuish et al. (2006). The MFCs implemented for this robotic setup were characterized by oxygen-diffusion based cathodes. This choice critically constrainted the maximum energy performance. Nevertheless, it was fundamental to provide the robots with a long term self-sustainable energy source, thus promoting the conditions for genuine energy autonomy. With respect to other MFC models currently available in the scientific literature, e.g. in Picioreanu et al. (2007) and Marcus et al. (2007), our model was intentionally built at a high level of abstraction. This allows us to capture the characteristic energy generation dynamic of a MFC without the burden of details that would be non-crucial for our robotic simulations. In its simple formulation, the model works as a plug-in that can be easily implemented on any robot platform in simulation, and can endow robotic agents with realistic MFC energy production dynamics with minimal and extremely limited computational overhead.

As we direct the reader to the exhaustive description of the model in Montebelli et al. (2010a), we will here specify the details for its full implementation. We essentially developed a simple *resistance-capacitance* (RC) model (Fig. 1). Two of its physical parameters, namely the electromotive force (V) and internal resistance (R_i) of the MFC, fully characterize the MFC as an electric generator. These parameters crucially depend on the level of hydration of the cathode and on the chemical energy available in the substrate biomass of the anodic chamber. This dependency was extracted using system identification techniques from the experimental data. Therefore, once provided with the current level of hydration and of substrate richness, the model simulates realistic MFC energy generation dynamics, quantitatively similar to the ones produced by 8 MFCs connected in series. With reference to Fig. 1, the electromotive force V generates the electric current that through the internal resistance R_i buffers energy in the external capacitor C. The presence of this latter element is an arbitrary choice of the robot designers at the BRL to endow the system with an energy reservoir. This gives a partial solution to the strong electric constraints deriving from the low power rates that typically emerge from a MFC. This part of the circuit, fully platform-independent, describes the *energy generation* process and is specifically addressed by the MFC model. As soon as the difference potential across the capacitor reaches an upper threshold ($Vc_{max} = 2.9V$) the electronic switch (S) is triggered and the energy stored in the capacitor is mobilized towards the robot sensors/actuators and to its control electronics. This second part of the circuit, described by the

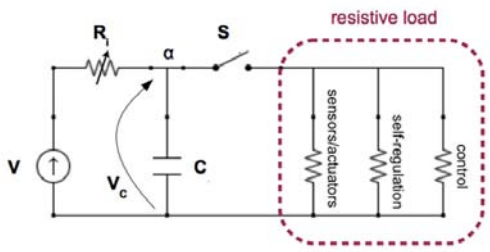

Figure 1: Electric schema of our model of energy generation in MFCs. The electromotive force (V) and the internal resistance (R_i) of the MFC depend on the current level of cathode hydration and on the biochemical energy in the substrate. This determines the dynamic of energy generation, buffered on the external capacitance (C). The dashed rectangle highlights the platform-dependent *resistive load*.

resistive load in Fig. 1, constitutes the *energy distribution* process and is completely platform-dependent. It cannot be addressed in general terms and must be tailored to the specific robot design. When the difference potential across the capacitor falls below a lower threshold ($Vc_{min} = 2.03V$) then the switch S is opened and the capacitor is recharged up to its upper threshold. This event closes the logical loop of the charge/discharge hysteresis cycle.

Using elementary electromagnetism we can describe the model in more analytical terms. The starting point is the first order linearly differential equation representing the electric current balance at node α in Fig. 1:

$$\frac{V - V_C}{R_i} = C\frac{dV_C}{dt} + I_M \tag{1}$$

where I_M represents the current drainage of the resistive load, while the meaning of all the other symbols has already been introduced. As anticipated, the quantity I_M, being platform-dependent, will be specified in the next section together with the other details regarding the specific robotic setup.

Under normal operating conditions, oxygen-diffusion cathode based MFCs are subject to water evaporation. Concurrently, although slower in time, the concentration of biochemical energy in the anodic substrate decays as a result of the bacterial activity. Linear laws describe the relations between: 1) the current level of hydration (hyd) and the time from the last full cathode hydration (t_h); 2) the chemical energy of the substrate ($subst$) and the time from the last anode replenishment with fresh substrate (t_s):

$$hyd = -\frac{t_h}{\tau_h} + 1 \tag{2}$$

$$subst = -\frac{t_s}{\tau_s} + 1 \tag{3}$$

where τ_h and τ_s (with $\tau_h << \tau_s$) respectively determine the time scales of the cathode dehydration and of the substrate biochemical energy decay.

The dependence of V and R_i with t_h is summarized by the following equations:

$$R_i = R_{i0} + k_{Ri}t_h \tag{4}$$

$$V = V_0 + k_V t_h \tag{5}$$

The effect of t_s is expressed by:

$$R_{i0} = q_R + m_R t_s \tag{6}$$

$$k_{Ri} = a_2 t_s^2 + a_1 t_s^1 + a_0 \tag{7}$$

$$V_0 = q_V + m_V t_s \tag{8}$$

The dynamic of R_{i0} is limited to values above 450. Numeric values for all the remaining symbols are: $C = 0.0282$, $k_V = -0.14$, $q_R = 642$, $m_R = -0.022$, $a_2 = 2.41e-8$, $a_1 = -1.1036e-4$, $a_0 = 0.1207$, $q_V = 3117V$, $m_V = -0.0166$, $\tau_h = 2500$, $\tau_s = 7000$ [1].

Finally, the energy currently stored in the capacitor (ε) can be easily derived from the current tension of the capacitor (V_C):

$$\varepsilon = \frac{1}{2}CV_C^2. \tag{9}$$

In conclusion, the differential equation 1, and equations 4–9 specify the model. Equations 2 and 3 allow the (equivalent) descriptions of the system in terms of time domain or as a function of the current levels of cathode hydration and substrate biochemical energy. According to this model, well hydrated MFC with fresh substrate can generate energy at a significantly higher rate than in dehydrated and 'starving' conditions. The system is particularly sensitive to the hydration level. A serious dehydration as well as an exhausted substrate determine the disruption of the charge-discharge cycle previously described and the energy generation mechanism collapses.

The robotic setup

In our experiments, a commercial *e-puck* robot simulated with the program Evorobot* (Nolfi and Gigliotta, 2010) could freely move in a square arena (measuring 1000 mm x 1000 mm), bound by opaque walls all around its perimeter (Fig. 2, central panel). Centrally located in the arena were two circular recharging areas (radius 120 mm). Upon entering in the lower circle, in whose center is placed a light source, the robot instantaneously received full cathode hydration (i.e. water was injected so to fill the capacity of its

[1] In order to limit the duration of each trial, we anticipated the kick in of the substrate effect by reducing the physical value of τ_s by a factor 3. Refer to Montebelli et al. (2010a) for details about the appropriate physical dimensions.

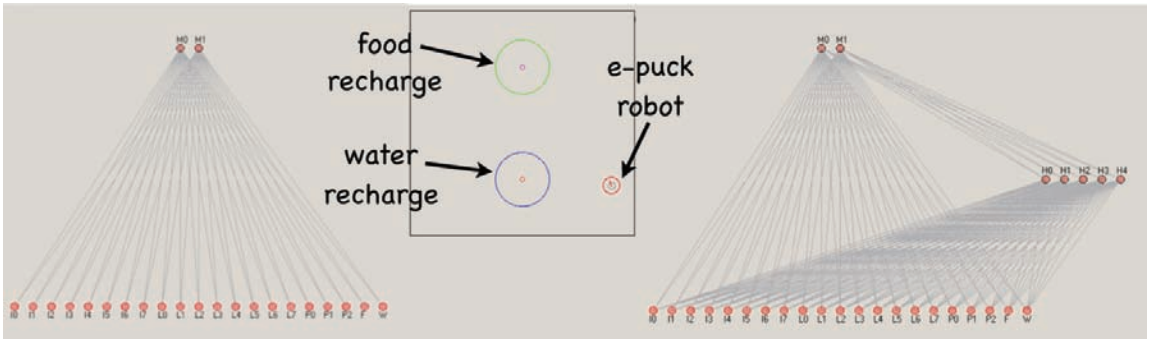

Figure 2: **Central panel-** Representation of the simulated arena. Upon entering the upper/lower circle (respectively, food/water recharging areas) the e-puck robot was fed with fresh substrate or fully rehydrated. **Left panel-** Feedforward ANN controller with no hidden layers. The ANN receives inputs from the robot's infrared and light sensors (I0-7 and L0-7), from its microphones (P0-2) and from the food and water level sensors (F and W). It outputs the motor activation signals of the robot's left and right motors (M0-1). **Right panel-** Feedforward ANN controller 5 hidden neurons and direct input-output connections.

cathode). On entering of the upper circle, landmarked by a continuous sound source, the robot received a complete and instantaneous refill of its anodic chamber with fresh substrate.

The simulated e-puck robot was provided with its standard 8 infrared sensors, 8 light sensors (activated by the light source) and 3 microphones (reacting to the sound source with an intensity that is inversely proportional to the square distance of the microphone from the sound source). A small quantity of noise was injected in the system. Customized water and food level sensors were included in the robot's sensory capabilities, providing information about the current level of cathode hydration and of the chemical energy stored in the anodic substrate.

The robot's motors were controlled by the activation of an artificial neural network (ANN). We tested several different standard architectures of discrete time ANNs, but in this report we will refer to only two of them for reasons of space. The first (Fig. 2, left panel) was a feedforward ANN with no hidden layer. The second (Fig. 2, right panel) was a feedforward ANN with five hidden neurons and direct input-output connections. In our setup, the robot's motor activation directly determined the energy drainage through the resistive load. The current I_M, i.e. the leakage term in equation 1, can be estimated as a function of the motor activation based on the robot's motor data sheets. Quantitatively:

$$I_M = 0.36|m_{act}| \tag{10}$$

where m_{act} is the current level of activation for each of the two motors, with values in the interval [-0.5 0.5], as imposed by the controlling ANN.

The energy production took place continuously (i.e. in any instant an electric current was flowing from the MFC to node α in Fig. 1) as long as the MFC was sufficiently hydrated and provided with fresh substrate. On the other hand, the energy distribution took the form of a hysteresis cycle. When the tension across the capacitor, V_C, reached its upper threshold an electric current flowed to power the robot's motors. When V_C fell below its lower threshold, the motor activity was suddenly inhibited and the robot remained still until V_C would be recharged above its upper threshold again. Accordingly, the current hydration level and the chemical energy of the substrate represent, in Ashby's terminology, the essential variables of the system.

We chose to boost the rate of energy generation characteristic of a series of 8 MFCs (the configuration that we used in order to identify the parameters of our MFC model) by a factor 100. That means that we considered a parallel electric connection of 100 elements constituted by 8 MFCs connected in series. Comments about this choice are left for the following discussion.

The free parameters of the ANN controller (synaptic weights and biases) were adapted in order to allow the robot to viably cope with its environment using a standard genetic algorithm (Goldberg, 1989) implemented in the Evorobot* simulator. We ran 10 replications of the evolutionary process, over 1500 generations with elitist selection. Each individual was on trial for 1000 simulated seconds (10000 time steps), and tested on 4 different trials from random starting position. The fitness function was intentionally rather generic: it integrated at each time step the absolute value of the current level of activation of the two motors, but only outside the recharging area. The rationale behind this choice was that we wanted the robot to consume the energy accumulated on its capacitor by demonstrating movement. On the other hand, similar to previous experiments by Floreano and Mondada (1996) and Montebelli et al. (2007, 2008), we wanted to avoid the affordance of clues about the existence of the light and sound sources, their relation to the recharging areas, their critical relations with the robot's hydration and food sensors, implicitly with the robot's energy generation rate and hence with its own overall viability.

We conclude this section with a few comments. Firstly, we emphasize the simplicity of our setup. A minimal setup focuses our attention on the object under study and allows a deeper mathematical exploration of the properties of the system. Secondly, in such a simple scenario a viable behavior might be imposed on the system by explicit design. Nevertheless, of all the options our choice was to adapt ANNs by using an evolutionary algorithm. The reason for our preference was twofold. On the one hand, we consider this alternative more liable to scaling up to more complex and less predictable circumstances (e.g. dynamically changing environments). On the other hand, we reckon on the flexibility of the fitness functions in evolutionary techniques for unsupervised adaptation, compared to other machine learning methods. This is functional to our focus on versatile robot autonomy within general and unpredictable environments, rather than on domain specific optimization.

Results

Continuous behavior

All of the considered ANN architectures managed to evolve viable behaviors for this simple task. In all cases the evolutionary process was liable to failures. Nevertheless, several classes of viable strategies were created during the evolutionary process for the best evolved individuals.

In the present and following sections we report the evolved behavior of the simplest control architecture that we considered, the feedforward ANN with no hidden layer sketched in Fig. 2, left panel. The *continuous* behavior of the best individual is shown in Fig. 3, left panel. The robot could move without sudden stops, as it would maintain a stable balance between the energy income from the MFC generator and the energy drained by its own motors (i.e. only seldom V_C fell below its lower threshold). The onboard capacitor provided a little energy buffer, but only episodically the robot had to stop and wait for its recharge.

During the initial transient period, the robot navigated in the environment, looking for a direct engagement with the water recharging area. Once reached its initial goal (Fig. 3, left panel), it maintained its engagement, looping around the water recharging area (associated with the light source) and systematically entering in it for hydration. After three loops around the light source, a fourth, larger loop would also encapsulate the food recharge area (marked by the sound source), entering which would instantaneously replenish the robot with fresh anodic substrate. This resulted in a stable and viable behavior: its timing maintained both essential variables within ideal bounds.

Essential variables as dynamic neuromodulators

By using a neuroscience-inspired clamp technique, similarly to Montebelli et al. (2008, 2009), we emphasized how the activation of the robot's water and food sensors was crucial for the emergence of the behavior. We clamped the values

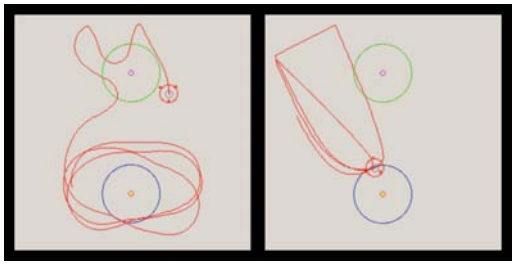

Figure 3: Examples of viable behaviors. After exhaustion of the initial transient, the robots enter in a stable, although not stereotypical loop, constituted of several passages across the water recharging area followed by one passage through the food area. **Left panel-** In the case of the continuos behavior generated by the ANN with no hidden layer (Fig. 2, left panel) the ratio between water and food access is $4:1$. **Right panel-** For the pulsed behavior of the ANN with hidden layer (Fig. 2, right panel) it is $3:1$. In both cases the trajectory of the robot is plotted for 1200 time steps.

of the two inputs F and W to arbitrary levels for the whole trial (i.e. we nullified the whole energy mechanism: the water and food levels remained constant at the selected value and the two recharging areas had no effect on the system). By systematically exploring different combinations of the clamped levels of hydration and substrate biochemical energy, we discovered that (after exhaustion of the transient period) these two essential variables, statistically determined the ratio between the numbers of accesses to water and food resources in the robot trajectories (*W:F ratio*). Ratios between $5:1$ and $1:1$ were observed (Fig. 4), and once mapped as a function of the values of the essential variables they showed a significant regularity (Fig. 5). In a tiny region of the essential variable state space, characterized by very high values of both F and W (both around 0.98), the system manifested bistability. The robot kept looping around either one or the other recharging area (Fig. 4, top and central right panels), depending on its starting position and on the integrated effects of noise. Behavioral transitions from one basin of attraction to the other were observed, although statistically rare (Fig. 4, bottom right panel). This persistence rapidly faded for different values of F and W, that modulated the height of the separation between the two different basins of attraction and the relative depth of the basins. For high values of F with subcritical levels of W (e.g. around 0.65) we noticed a maximal bias towards water, and accordingly a higher W:F ratio. Finally, in the vast area where the ratio is mapped to 0, we observed nonviable monostable behaviors, i.e. the robot would remain on a single behavioral attractor, without systematically entering any of the two recharging areas.

Detailing how the two essential variables (directly related to realistic MFC dynamics) modulated the behavioral dy-

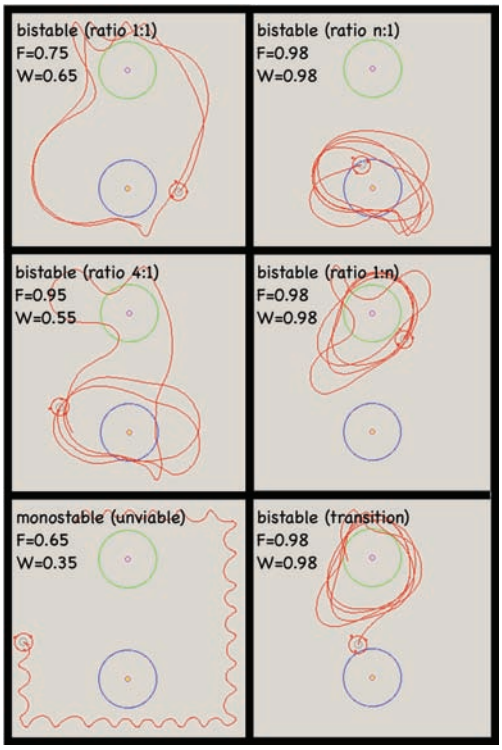

Figure 4: Examples of robot trajectories (behavioral attractors), for different clamped values of inputs W and F as specified on each panel, demonstrate different water to food access ratios. **Top and central left panels-** Examples of ratio $1:1$ and $4:1$. **Bottom left panel-** Unviable behaviors dominate lower levels of activation of the W and F sensors. **Top and central right panels-** Local behavioral attractors in the bistable regime. **Bottom right panel-** Random transition from one behavioral attractor to the other.

namics of this simple and purely reactive neurocontroller constitutes the main and novel practical contribution of this work. During normal interactions with its environment (the evolved task) the system relies on a *dynamic action selection mechanism*, self-organized during evolution without any hardwired rule.

Continuous vs. pulsed behavior

The behavior of the robot analyzed in the previous sections will here be compared to a qualitatively different *pulsed* behavior observed in the case of the feedforward ANN with 5 hidden neurons and direct input/output connections (Fig. 2, right panel). The robot always moved at its maximal speed, thus draining more energy than instantaneously provided by the MFC generator. Therefore, it systematically exhausted the energy stored on the capacitor and exploited the energy distribution hysteresis cycle previously described.

As in the previous case, the best evolved individual moved towards the water recharging area first. Once its stable behavior is reached, the robot engaged in regular loops from the water recharging area to the wall on the left side of the arena and back to the recharging area (Fig. 3, right panel). Every two loops, a third loop would emerge with a broadened width encapsulating the food recharging area. The robot apparently acted by integrating the information from all its sensory modalities. This behavior also qualifies as stable and viable, actually performing across the different trials equally well as the continuous behavior.

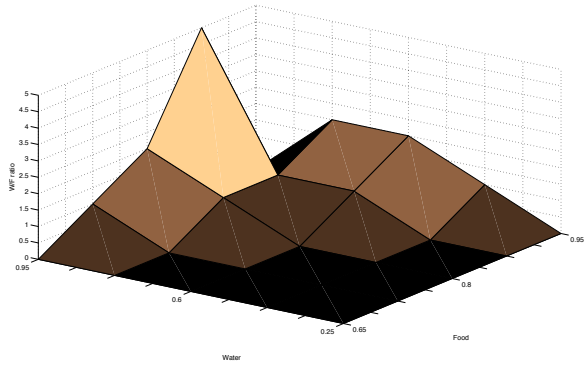

Figure 5: Water to food-access ratio (*W:F ratio*) as a function of the essential variables W and F. The area hidden under the highest peak is a region of bistability characterized by rare transitions between the two attractors. The dark area with 0 ratio represents dysfunctional behaviors: the robot cannot maintain its essential variables within a viable region.

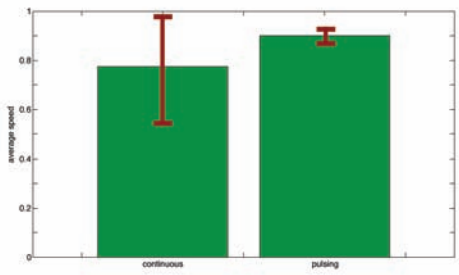

Figure 6: Average and standard deviation for the absolute value of the motor activation during continuous and pulsed behavior. Data from 2000 time steps of actual movement.

Fig. 6 quantitatively demonstrates the different nature of the continuous and pulsing behaviors. The continuously moving agent had its motors activated at about 77% of their maximal speed, with high variability, as demonstrated by the plot of the standard deviation. On the other hand, considering only the time intervals during which the robot was actually moving, the pulsing behavior was performed at 91% of the motor speed maximum, with a very low standard deviation.

Discussion

One of the most intriguing properties of computer simulations is the possibility to anticipate the forcefully slow pace of technological progress. As such, it should be used with full awareness and attention. In our study we multiplied by a factor 100 the basic electric performances of the modeled MFC energy generator. There are at least two important justifications for this choice. The first is experimental: preliminary studies (Ieropoulos et al., 2008) produced significant evidence that smaller MFCs might generate energy more efficiently, i.e. with a higher level of energy density. The second is theoretical, as it has been argued that the implementation of micron-level biofuel cells is possible in principle, and prototypes have been implemented (Kim et al., 2003). Although more research is necessary, the progressive miniaturization of MFCs seems to suggests an extremely alluring future scenario. With our choice of the multiplicative factor we anticipated the possibility to carry on board of our simple robot 800 single MFCs. The state of the art prototype of MFC powered robot, EcoBot-III, is currently endowed with a stack configuration of 48 basic MFCs. This number, limited for obvious practical reasons, is nevertheless destined to grow. Following these considerations, the factor 20 between the current physical implementation and our simulation seems appropriate.

This said, the selected multiplicative factor endowed our work with the power to foresee a crucial bifurcation in the development of MFC technology for robotic applications. The prospective historical period on which our investigation resides is the moment of transition from pulsed to continuos behaviors in MFCs powered robots. In other words, the moment when enough power is generated in order to support a sub-maximal motor activation in continuous mode. This is not to rule out the possibility of interesting pulsed behaviors. As already mentioned in Melhuish et al. (2006), for more complex cognitive architectures and environments, the intervals of stillness during energy recharge might be the perfect place to start dealing with cognition in terms of planning for thoughtful action selection, where 'mental activity' might be energetically less demanding than actual overt behavior. A similar approach, although still at a larval phase of development has been considered by Lowe et al. (2010). In this novel work, during the idle motor intervals, the robot can capitalize on active 'sensing' by executing energetically inexpensive visual saccades, rather than actual physical navigation.

Finally, why should we abandon the engineering perspective of robots that could turn to virtually unlimited sources of energy (in form of power sockets or batteries), a perspective largely inherited by cognitive roboticists? As a matter of fact, we just analyzed a not even too futuristic scenario where MFCs will converge towards offering the MFC powered robots the option of continuous action, simply considering appropriate stack configurations of basic miniaturized MFCs. Furthermore, if pragmatic results will support the theoretical expectations, MFC miniaturization might create a sort of limit situation, allowing a fully distributed energy generation system reminiscent of biological cellular energy generation strategies, where energy constrains would be crucially relaxed. A serious answer to this question has to do with our idea of autonomy. Future MFC powered robotic agents, through the development of a viable behavior in their environment, will be ecologically rooted in their environmental context. They will depend on food and water resources that are available as long as the robots can live in a sustainable and meaningful 'ecological relation' to their environment. This property, novel and original in robotics, represents an exciting new scenario for future research.

Conclusions

This work, jointly with the mentioned paper by Lowe et al. (2010), represents the first effort aimed to put to the test the MFC model for robotic simulations presented in Montebelli et al. (2010a). Its aim, beyond the mere demonstration, is to ground previous work related to the dynamic neuromodulatory role of non-neural internal variables (Montebelli et al., 2007, 2008) in a realistic simulation of physical energy constraints. The robot is energetically autonomous insofar as it can sustain a viable interaction with its environment by maintaining its essential variables. Within this tight agent-environment interaction, our analysis emphasized the neuromodulatory role played by the essential variables for dynamic action selection with no hardcoded rules. We also pointed to the possible coexistence of several viable strategies, different both in qualitative and quantitative terms and to their possible cognitive implications in a novel scenario of 'ecologically grounded' energy and motivational autonomy.

In future work we will further investigate these findings. The *2 resource problem* has been characterized in McFarland and Spier (1997), where a robot was expected to negotiate between an environmental resource critical to its survival (fuel) and the execution of a task that some external supervisor considered useful (work). We are extending our experimental setup for a fully fledged *3 resource problem*, where the exploitation of food and water will be functional to the execution of physical work in a dedicated area. In addition the experimental setup appears suitable for a deeper exploration of the concept of *embodied anticipation* (i.e. the capacity to profit from the non-neural neuromodulatory characteristics achieved during evolutionary and ontogenetic adaptation in order to perform swift readaptation to novel situations) as proposed in Montebelli et al. (2009, 2010b).

Acknowledgements

This work has been supported by a European Commission grant to the project *"Integrating Cognition, Emotion and Autonomy"* (www.iceaproject.eu, IST-027819 - 2006-2009).

References

Ashby, W. R. (1960). *Design for a Brain: The Origin of Adaptive Behavior*. John Wiley & Sons Inc., New York, NY.

Avila-García, O. and Cañamero, L. (2004). Using hormonal feedback to modulate action selection in a competitive scenario. In Schaal, S., Ijspeert, A., Billard, S., and Vijayakumar, J., editors, *Proceedings of the Eighth International Conference on Simulation of Adaptive Behaviour*, 243–252, Cambridge, MA. MIT Press.

Cannon, W. B. (1915). *Bodily Changes in Pain, Hunger, Fear and Rage*. Appleton, New York.

Di Paolo, E. (2003). Organismically-inspired robotics. In Murase, K. and Asakura, T., editors, *Dynamical Systems Approach to Embodiment and Sociality*, 19–42. Advanced Knowledge International, Adelaide.

Floreano, D. and Mondada, F. (1996). Evolution of homing navigation in a real mobile robot. *IEEE Transactions on Systems, Man and Cybernetics, Part B*, 26(3):396–407.

Goldberg, D. E. (1989). *Genetic Algorithms in Search, Optimization, and Machine Learning*. Addison-Wesley Professional.

Ieropoulos, I., Greenman, J., and Melhuish, C. (2008). Microbial fuel cells based on carbon veil electrodes. *International Journal of Energy Research*, 32:1228–1240.

Ieropoulos, I., Melhuish, C., and Greenman, J. (2007). Artificial gills for robots. *Bioinspiration and Biomimetics*, 2:S83–S93.

Kim, H.-H., Mano, N., Zhang, Y., and Heller, A. (2003). A miniature membrane-less biofuel cell operating under physiological conditions at 0.5v. *Journal of the Electrochemical Society*, 150:A209/A213.

Logan, B. E., Hamelers, B., Rozendal, R., Schröder, U., Keller, J., Freguia, S., Aelterman, P., Verstraete, W., and Rabaey, K. (2006). Microbial fuel cells: Methodology and technology. *Environmental Science and Technology*, 40(17):5181–5192.

Lowe, R., Montebelli, A., Ieropoulos, I., Greenman, J., Melhuish, C., and Ziemke, T. (2010). Grounding Motivation in Energy Autonomy: A Study of Artificial Metabolism Constrained Robot Dynamics. In *Proceedings of the 12th International Conference on the Synthesis and Simulation of Living Systems*, in press.

Lowe, R., Nehaniv, C. L., Polani, D., and Cañamero, L. (2005). The degree of potential damage in agonistic contests and its effects on social aggression, territoriality and display evolution. In *Proceeding of the Congress on Evolutionary Computation - IEEE CEC '05*, vol 1, 351–358.

Marcus, A. K., Torres, C. I., and Rittmann, B. E. (2007). Conduction-based modeling of the biofilm anode of a microbial fuel cell. *Biotechnology and Bioengineering*, 98(6):1171–1182.

McFarland, D. and Spier, E. (1997). Basic cycles, utility and opportunism in self-sufficient robots. *Robotics and Autonomous Systems*, 20:179–190.

McHale, G. and Husbands, P. (2006). Incorporating energy expenditure into evolutionary robotics fitness measures. In et al., L. M. R., editor, *Proc. Alife X*, 206–212. MIT Press.

Melhuish, C., Ieropoulos, I., Greenman, J., and Horsfield, I. (2006). Energetically autonomous robots: food for thought. *Autonomous Robots*, 21:187–198.

Moioli, R. C., Vargas, P. A., von Zuben, F. J. V., and Husbands, P. (2008). Towards the evolution of an artificial homeostatic system. In *IEEE Congress on Evol. Comput.*, 4024–4031.

Montebelli, A., Herrera, C., and Ziemke, T. (2007). An analysis of behavioral attractor dynamics. In Almeida e Costa, F., editor, *Advances in Artificial Life: Proceedings of the 9th European Conference on Artificial Life*, 213–222, Berlin. Springer.

Montebelli, A., Herrera, C., and Ziemke, T. (2008). On cognition as dynamical coupling: An analysis of behavioral attractor dynamics. *Adaptive Behavior*, 16(2-3):182–195.

Montebelli, A., Ieropoulos, I., Lowe, R., Melhuish, C., Greenman, J., and Ziemke, T. (2010a). Unplugged! a mathematical model of microbial fuel cells for energetically self-sustainable simulated robotic agents. *In preparation*.

Montebelli, A., Lowe, R., and Ziemke, T. (2009). The cognitive body: from dynamic modulation to anticipation. In Pezzulo, G., Butz, M. V., Sigaud, O., and Baldassarre, G., editors, *Anticipatory Behavior in Adaptive Learning Systems*, 132–151. Springer, Berlin, Heidelberg.

Montebelli, A., Lowe, R., and Ziemke, T. (2010b). More from the body: Embodied anticipation for swift re-adaptation in neurocomputational cognitive architectures for robotic agents. In Gray, J. and Nefti-Meziani, S., editors, *Advances in Cognitive Systems*, in press. IET.

Nolfi, S. and Gigliotta, O. (2010). Evorobot*. In Nolfi, S. and Mirolli, M., editors, *Evolution of Communication and Language in Embodied Agents*, 297–302. Springer-Verlag, Berlin, Heidelberg.

Parisi, D. (2004). Internal robotics. *Connection Science*, 16(4):325–338.

Pfeifer, R. and Scheier, C. (1999). *Understanding Intelligence*. MIT Press, Cambridge, MA.

Picioreanu, C., Head, I. M., Katuri, K. P., van Loosdrecht, M. C. M., and Scott, K. (2007). A computational model for biofilm-based microbial fuel cells. *Water Research*, 41:2921–2940.

Saglimbeni, F. and Parisi, D. (2009). Input from the external environment and input from within the body. In Kampis, G. and Szathmary, E., editors, *The 10th European Conference of Artificial Life*, Berlin. Springer.

Wilson, M. (2002). Six views of embodied cognition. *Psychonomic Bulletin and Review*, 9(4):625–636.

Ziemke, T. (2003). What's that thing called embodiment? In Alterman, R. and Kirsh, D., editors, *Proc. of the 25th annual conference of the Cognitive Science Society*, 1305-1310. Lawrence Erlbaum.

Ziemke, T. (2008). On the role of emotion in biological and robotic autonomy. *BioSystems*, 91:401–408.

Ziemke, T. and Lowe, R. (2009). On the role of emotion in embodied cognitive architectures: From organisms to robots. *Cognitive computation*, 1(1):104–117.